Physics – Uspekhi **55** (7) 721 – 738 (2012)

CONFERENCES AND SYMPOSIA

PACS numbers: 01.10.Fv, **02.70.–c**, **05.10.–a**, **05.50.+q**, 14.60.St, **23.40.–s**, **31.10.+z**, 42.55.Lt, 42.60.Lh, 52.50.Jm

Modern problems in the physical sciences (Scientific session of the Physical Sciences Division of the Russian Academy of Sciences, 23 November 2011)

DOI: 10.3367/UFNe.0182.201207g.0773

On 23 November 2011, the scientific session of the Physical Sciences Division of the Russian Academy of Sciences (RAS) was held at the conference hall of the Lebedev Physical Institute, RAS.

The following reports were put on the session agenda posted on the website www.gpad.ac.ru of the RAS Physical Sciences Division:

(1) **Ionin A A** (Lebedev Physical Institute, RAS, Moscow) "High-power infrared and ultraviolet lasers and their applications";

(2) **Romanovskii M Yu** (Prokhorov General Physics Institute, RAS, Moscow) "Laser-induced acceleration of the forbidden captures of orbital electrons by nuclei";

(3) **Petrukovich A A** (Space Research Institute, RAS, Moscow) "Earth's magnetosphere as a plasma laboratory";

(4) **Shchur L N** (Landau Institute for Theoretical Physics, RAS, Chernogolovka, Moscow region) "Computational physics and the verification of theoretical predictions".

Articles written on the base of oral reports 1, 2, and 4 are published below.

PACS numbers: 42.55.Lt, 42.60.Lh, 52.50.Jm
DOI: 10.3367/UFNe.0182.201207h.0773

High-power IR- and UV-laser systems and their applications

A A Ionin

1. Introduction. A brief historical outline of studies made at the Laboratory of Gas Lasers at the Lebedev Physical Institute

The term 'high-power' laser is quite vague, especially for pulsed lasers with high peak powers. For cw and repetitively pulsed high-power lasers, the lower range limit can be conditionally accepted to be ~ 1 kW of average output power, while this limit for pulsed lasers can be estimated by the peak power of ~ 1 MW. The maximum average power has been achieved in megawatt lasers [1], while the maximum peak power of about 1 PW has been generated in femtosecond laser pulses [2]. At present, femtosecond pulsed lasers with peak powers of up to ~ 10 PW are being developed, and the possibility of creating exawatt pulsed lasers is being discussed [2]. In this paper, mainly IR and UV lasers developed, investigated, and exploited in studying the interaction of radiation with matter at the Laboratory of Gas Lasers (LGL) at the Lebedev Physical Institute, RAS (FIAN in *Russ. abbr.*) with the participation of the author are considered.

The Laboratory was founded by N G Basov (1922–2001) in the early 1980s for studying the physical principles of exploring high-power industrial and defense-purposes lasers. Researchers at the Laboratory took part in the development of a megawatt class CO_2 laser [1] and 10–30-kW average-power industrial CO_2 and CO lasers. The main avenues of research conducted at the LGL are the development of excimer lasers, atomic-transition lasers, molecular lasers, and the interaction of laser radiation with matter.

Researchers at the LGL have created a variety of large-scale lasers, such as an electron-beam-pumped KrF laser (under the supervision of V D Zvorykin) with an active volume of about 20 l emitting 0.248-μm, 100-J, 100-ns pulses; electron-beam-pumped and electron-beam-controlled atomic transition pulsed lasers (under the supervision of I V Kholin) comprising a 1.73-μm, 80-J Ar/Xe laser, 1.27-μm, 4.5-J He/Ar laser, 2.52-μm, 4-J He/Kr laser, and 0.58-μm, 1.5-J He/Ne laser; and pulsed electron-beam-controlled molecular lasers (under the supervision of the author of this paper) comprising a 10.6-μm, 500-J CO_2 laser, a fundamental-transition 5–6-μm, 800-J CO laser and overtone-transition 3-μm, 50-J CO laser, an N_2O laser ($\lambda = 10.9$ μm, $Q = 100$ J), and a quasi-cw supersonic 100-kW CO laser emitting 1-ms pulses [4]. A group of researchers at the Laboratory headed by B I Vasil'ev have proposed the scheme and developed the design of a two-frequency differential-absorption lidar, in which the reference beam is formed by radiation from a CO_2 laser and the operating-beam radiation can be sequentially tuned over lines in the spectrum of an NH_3 laser [3].

The Laboratory of Gas Lasers at FIAN has actively collaborated and continues to collaborate with foreign institutions in the advancement of laser technologies. In 1992–1996, researchers of the Laboratory were involved, together with colleagues from Great Britain and France, in the Eureka-113 CO-Eurolaser European project [5] on the development of high-power industrial CO lasers. In 1994, researchers at the Institute of Technical Physics (Stuttgart,

A A Ionin Lebedev Physical Institute, Russian Academy of Sciences, Moscow, Russian Federation
E-mail: aion@sci.lebedev.ru

Uspekhi Fizicheskikh Nauk **182** (7) 773 – 792 (2012)
DOI: 10.3367/UFNr.0182.201207g.0773
Translated by V I Kisin, Yu V Morozov, M Sapozhnikov; edited by A Radzig

Uspekhi Fizicheskikh Nauk **182** (7) 773 – 781 (2012)
DOI: 10.3367/UFNr.0182.201207h.0773
Translated by M Sapozhnikov; edited by A Radzig

Germany), in collaboration with research workers from the LGL, put into service a repetitively pulsed CO laser operating at room temperature with an average of about 1-kW output power [6]. In 1995–1998, the Laboratory participated in the Eureka-1390 Ultralas European project (Russia, Austria, Germany, and some others) aimed at the establishment of principles for the construction of a 100-kW industrial CO_2 laser.

In 1995–1996, together with colleagues at the Directorate of Applied Technology, Test and Simulation (DATTS) (White Sands proving ground, USA) and using the equipment brought by them, researchers at the LGL investigated the phase conjugation for radiation from CO_2 and CO lasers created at the LGL [7]. The same lasers were used in 1995–1997 in the team work with DuPont (Wilmington, USA) on the laser modification of the surface of synthetic fabrics by exposing the surface of nylon and Dacron fibers to frequency-selective radiation from a CO laser at a wavelength of ≈ 6 μm to eliminate so-called synthetic gloss [8], and in 1997–1999 for collaborative studies with the Colorado School of Mines (Golden, USA) on the interaction of radiation from high-power IR lasers with oil-bearing rocks [9], within the framework of a project on estimating the possibility of the manufacture of laser drilling rigs.

Later projects on developing, along with the University of New Mexico and the Air Force Research Laboratory (AFRL) (Albuquerque, USA), a supersonic CO laser operating on fundamental and overtone transitions in the CO molecule and studying electric-discharge generators of a singlet-oxygen energy donor for an oxygen–iodine laser and an electric discharge controlled by combined femtosecond and nanosecond UV pulses from a hybrid KrF-laser system, which were supported by partnership projects of the International Science and Technology Center (ISTC) with the European Office of Aerospace Research & Development (EOARD), are discussed in Sections 2–5.

2. Infrared carbon monoxide lasers and their application

Carbon monoxide (CO) lasers [which should be distinguished from carbon dioxide (CO_2) lasers] are of interest both for the creation of high-power mid-IR coherent radiation sources and for studying molecular kinetics, because the population inversion between the vibrational–rotational levels of the CO molecule is produced due to the vibrational–vibrational energy exchange between CO molecules which constitute pronounced anharmonic oscillators. The CO laser can emit at $\sim 10^3$ vibrational–rotational spectral lines in fundamental vibrational bands with a change in the vibrational quantum number by unity in the spectral range from 4.6 to 8.2 μm and at the first overtones in the wavelength range from 2.5 to 4.2 μm. The history of the advent and evolution of CO lasers and the physical principles of their operation (in particular, the reasons for the necessity of cooling the active medium of the laser) are presented in review [10].

The emission region of an overtone CO laser covers 'the transparency window' of the terrestrial atmosphere in the wavelength range from ≈ 3.3 to 4.0 μm, and therefore this laser can be utilized for the transport of high-power radiation in the atmosphere. Because a huge number of the emission lines of the CO laser lie in spectral regions where the absorption lines of many explosives and toxic substances are located, CO lasers, not necessarily with high output powers, can be used for a multicomponent gas analysis of these and other substances.

Research into CO lasers at the LGL has been concentrated during the last decade on the following areas: the creation and exploration, in joint work with colleagues from the USA, a supersonic CO laser, in particular, an overtone laser; the development of a compact CO laser tunable in the 5-μm wavelength range and emitting at overtone transitions in the region from 2.5 to 4.0 μm upon pumping by a high-frequency (radio-frequency or RF) slab discharge; the creation of a CO-laser system generating nanosecond pulses; and the estimation of the possibility of CO laser applications for laser uranium isotope separation.

2.1 Supersonic overtone CO laser

A supersonic overtone CO laser with the active medium cooled during its adiabatic expansion in a supersonic nozzle was developed and investigated within the framework of collaborative ISTC projects Nos 1865 and 2415 based on recommendations formulated at the LGL, where the operation of the supersonic CO laser launched at the AFRL was simulated theoretically and experimentally. These studies have revealed that the overtone CO laser can emit in high-lying vibrational bands, up to the $38 \to 36$ transition, at more than 400 spectral lines in the selective mode and with an efficiency up to 16% in the multifrequency mode (see, for example, Ref. [11]). The setup at the AFRL was initially constructed based on a high-frequency-discharge-pumped supersonic CO laser with an output power of 330 W (with a single-pass cavity) developed at the Institute of Technical Physics in Stuttgart. The design of the setup was considerably changed in collaborative work with American and German colleagues [12] by retaining its active volume (the active length measured 10 cm, the Mach number in a supersonic flow reached 2.7, the gas temperature and pressure in the stream were ≈ 100 K and 2–9 Torr, respectively, and the output power at fundamental transitions (≈ 5 μm) achieved 2.1 kW with an efficiency of 21% (for a single-pass cavity). For overtone transitions, 50 W of output power were achieved in the case of highly reflecting mirrors. Estimates showed that the output power of an overtone CO laser with the optimal cavity can approach 500 W.

2.2 High-frequency-discharge-pumped compact slab CO laser

Recently, considerable progress has been achieved in the advancement of diffusion-cooled capillary and slab gas lasers (including gas-flow and sealed CO_2 and CO lasers) excited by a capacitive transverse RF discharge. In these lasers, heat is removed from a gas mixture through cooled electrodes to which the exciting high-frequency voltage is applied. The RF discharge offers a number of advantages compared to the simple and often used dc discharge. The CO laser is known to demonstrate the highest output characteristics at cryogenic temperatures of the active gas mixture. This is especially inherent in the overtone CO laser [13]. An important practical problem consists in the development of a compact RF discharge-pumped slab CO laser with the active medium diffusively cooled to low temperatures. Such a laser, combining relative simplicity and compactness inherent in slab RF designs and the high efficiency and a broad emission spectrum typical of electric-discharge CO lasers, can become a unique spectroscopic tool for detecting various explosives, toxics, and other hazardous substances and materials.

Researchers at the LGL have developed compact RF-discharge pumped slab CO lasers with cryogenically cooled electrodes and different active-medium lengths (250 and 400 mm) [14]. Optimal conditions (the gas-mixture composition and pressure, RF discharge parameters) were established for obtaining the best laser output characteristics. The maximum mean power output of the fundamental-transition CO laser (in the spectral range from 5.1 to 5.4 μm) was $\approx$ 12 W, with the efficiency achieving $\approx$ 14%. This laser can also operate in the frequency-selective mode. Single-frequency lasing was observed at approximately 100 spectral lines in the wavelength range from 4.9 to 6.5 μm with a mean power output from a few milliwatts to a few dozen milliwatts. Researchers at the LGL have obtained for the first time lasing in an RF-discharge pumped slab cryogenic CO laser at overtone transitions in the CO molecule in the spectral range from 2.5 to 4.0 μm [14].

By optimizing experimental parameters in the free-running multifrequency lasing regime, the author of this paper, together with A Yu Kozlov, L V Seleznev, and D V Sinitsyn (FIAN), has recently achieved a mean power of $\approx$ 1.8 W in the spectral range from 2.95 to 3.45 μm, with an efficiency up to 1.5%. All the results were produced without the forced replacement of a gas mixture. Under fixed experimental conditions, stable lasing (with output characteristics fluctuating within 10%) was obtained in the time interval exceeding an hour, which demonstrated for the first time the operation of a cryogenic CO laser in the sealed mode. The tuning range of the CO laser overlaps the spectral regions comprising the absorption lines and bands of usual substances (H_2O, CO_2, O_3, N_2O, NO_2, NO, SO_2, NH_3, etc.), organic compounds (methane, acetone, benzene, methanol, ethanol, etc.), and strong contaminants.

A CO laser operating on many spectral lines is an attractive radiation source for spectral analysis of multicomponent gas mixtures and individual substances present in the atmosphere. The overtone CO laser was used in model experiments on measuring the concentration of gases in the two-component mixture ($N_2O + CH_4$) in the region of the overlap of their absorption spectra (Fig. 1). It was demonstrated that the accuracy of recovering the concentration of gases in a multicomponent mixture increased upon increasing the number of laser lines involved in measurements.

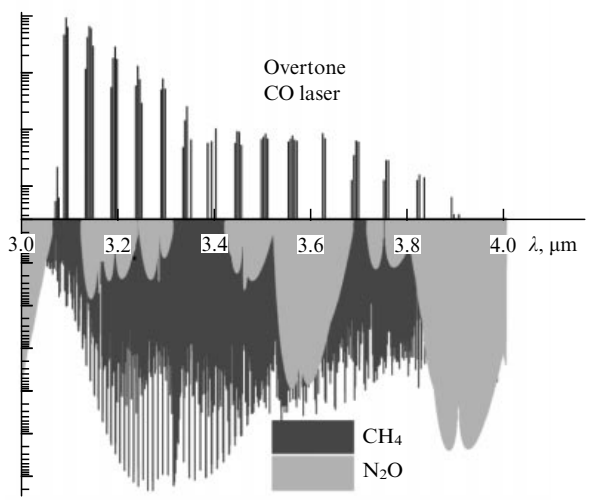

Figure 1. Typical emission spectrum of an overtone CO laser and absorption spectra of methane (CH_4) and nitrous oxide (N_2O).

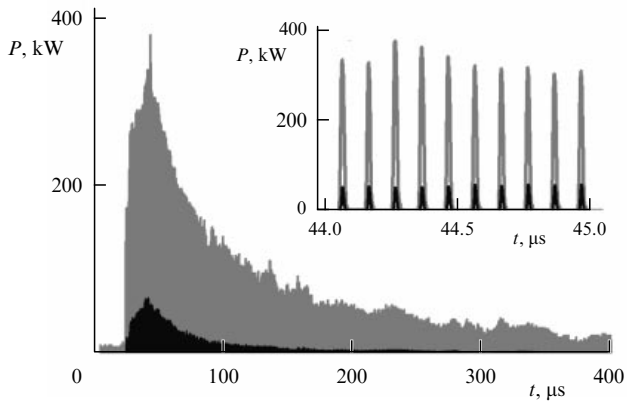

Figure 2. Train of nanosecond pulses at the input (dark color) and output (grey color) of the CO laser amplifier.

2.3 Nanosecond master oscillator–laser amplifier CO laser system

The laser levels of the CO molecule are populated due to a comparatively slow vibrational energy exchange between colliding molecules, and therefore it was assumed until recently that the mode-locked CO laser operating on vibrational–rotational transitions exhibits a low efficiency. However, high-power nanosecond pulses at $\sim$ 5 μm proved to be required for solving the complex scientific and technical problem of stochastic cooling of relativistic ions in colliders. It was demonstrated in paper [15] that our electron–beam-controlled, actively mode-locked, cryogenic CO laser could generate a train of 5–15-ns pulses at a repetition rate of 10 MHz, equal to the repetition rate of ion bunches in the RHIC (Relativistic Heavy Ion Collider) at the Brookhaven National Laboratory (USA). The peak power output of this laser achieved 120 kW in the multifrequency mode ($\approx$ 29 spectral lines), and 70 kW in the frequency-selective mode for lasing at the $9 \rightarrow 8P(11)$ transition line. The output peak power of the CO laser was increased to 380 kW in the multifrequency mode (Fig. 2) and to 130 kW in the frequency-selective mode by employing a specially developed master oscillator–laser amplifier system [16]. The study of the amplification of short laser pulses gave evidence that, due to the high rotation relaxation rate, the gain saturation intensity at a spectral line in the CO laser amplifier was $\approx$ 14 kW cm^{-2}, which exceeds the gain saturation intensity in a multifrequency cw CO laser by a few orders of magnitude.

2.4 Uranium isotope separation by means of CO lasers

Until recently, the CO laser was considered only as a promising radiation source for exciting photochemical reactions accompanying the separation of uranium isotopes, because several lines of this laser near $\lambda = 5.3$ μm fall into the $3\nu_3$ absorption band of uranium hexafluoride (UF_6) molecules [17] and can isotope-selectively initiate chemical reactions [18]. However, the situation changed dramatically when it was shown that short pulses from a mode-locked CO laser have a high peak power [15, 16] and, therefore, can be converted in nonlinear optical crystals to other spectral ranges. For example, the internal second-harmonic conversion coefficient for the CO-laser radiation in a $ZnGeP_2$ crystal achieved 25% [19, 20], which confirms the possibility of the efficient radiation frequency conversion by summation and subtraction of the CO-laser radiation frequencies. All the more because the CO laser can emit approximately 1000 lines

in the frequency-selective mode in a wide wavelength range from 2.5 to 8.3 μm. Due to such unique properties, CO-laser radiation can be converted to fall to the absorption bands of uranium hexafluoride molecules wherein the isotope shift is present, which is necessary for the laser separation of uranium isotopes, including the ν_3 band with the high absorption cross section near 16 μm [17]. Thus, the CO laser with radiation conversion in nonlinear optical crystals can become the efficient radiation source for uranium isotope separation.

3. Problem of the development of an electric-discharge IR oxygen–iodine laser

Chemical oxygen–iodine lasers (COILs) utilize singlet oxygen molecules $O_2(a^1\Delta_g)$ as energy donors for atomic iodine emitting laser radiation. However, the application of COILs is restricted due to the necessity of using toxic substances for obtaining singlet oxygen molecules in a chemical generator. One of the alternative methods for generating singlet oxygen is its production in an electric discharge. Lasing in the electric-discharge oxygen–iodine laser was first obtained by exciting an oxygen-containing gas mixture and producing singlet oxygen in a radio-frequency discharge, which was followed by mixing singlet oxygen in a laser mixture with iodine and cooling the mixture in a supersonic flow [21]. Singlet oxygen has been produced in an electric-discharge singlet-oxygen generator. Then, the singlet oxygen is transported to a region of mixing with iodine atoms supplied by iodine-containing molecules. Lasing at a wavelength of 1.316 μm appears directly after mixing singlet oxygen with atomic iodine in the laser cavity. The cooling of the gas mixture to cryogenic temperatures provides a positive gain for a considerably smaller singlet-oxygen yield $Y = [O_2(a^1\Delta_g)]/([O_2(X^3\Sigma_g^-)] + [O_2(a^1\Delta_g)])$, approaching $Y_{th} \approx 1\%$ at $T = 100$ K. For comparison, $Y_{th} \approx 15\%$ at $T = 300$ K. (The physics and techniques of producing singlet oxygen in an electric discharge, in particular, in a radio-frequency discharge, are described in detail in review [22].) At present, the maximum power output of the electric-discharge oxygen–iodine laser equals ≈ 500 W [23]. The U.S. Defense Advanced Research Projects Agency (DARPA) supports projects on the creation of a 100-kW oxygen–iodine laser with a lasing efficiency of ≈ 10% [24].

Experimental studies on the energy characteristics of an electric singlet-oxygen generator based on a pulsed e-beam sustained discharge in oxygen-containing gas mixtures showed that the addition of CO or H_2 to a gas mixture of O_2 and Ar considerably improved the stability of the discharge, providing a high specific energy input (the maximum value recalculated to the molecular components of the mixture reached ≈ 6.5 kJ l^{-1} atm^{-1} (≈ 150 kJ mol^{-1}) in the O_2:Ar:CO gas mixtures (1:1:0.1) at a total gas pressure of 30 Torr and an excitation volume of about 18 l [25]). It was predicted theoretically that, by using mixtures with CO, H_2, or D_2 molecular additions in an e-beam sustained discharge, one can expect a yield of singlet oxygen $O_2(a^1\Delta_g)$ reaching approximately 25%, which exceeds the value required for the operation of the oxygen–iodine laser at room temperature [25].

To study the production and relaxation of singlet oxygen molecules in a subsonic gas flow excited by a transverse slab radio-frequency discharge, an original experimental setup was developed within the framework of collaborative ISTC project No. 3835 (Fig. 3). Experimental results and numerical simulations [26] suggest that it is possible to obtain lasing in the oxygen–iodine laser with an electric-discharge singlet-oxygen generator based on a transverse RF discharge upon cooling the excited gas down to ≈ 220 K, which is quite real even without the employment of a supersonic expansion of the gas flow.

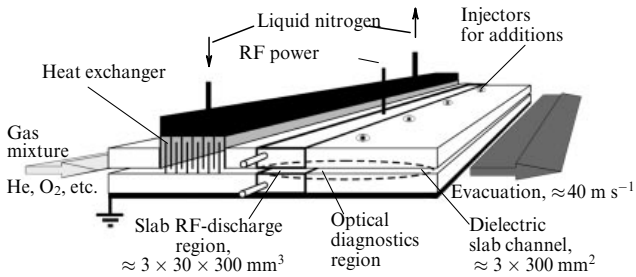

Figure 3. Schematic of an electric-discharge singlet-oxygen generator based on a gas-flow slab setup with transverse radio-frequency excitation and the possibility of the cryogenic cooling of electrodes.

4. The hybrid system of UV Ti:Sa–KrF lasers

To study the interaction of femtosecond laser pulses with matter, researchers at the LGL developed a hybrid solid-state–gas laser system [27] consisting of a Ti:Sa start-up laser and electron-beam KrF laser amplifiers built earlier (see the Introduction and Ref. [3]). A specific feature of hybrid systems is that femtosecond pulses generated by a solid-state laser and passed through a prism stretcher with negative dispersion are directly amplified in gaseous active media without recourse to the complicated and expensive optical compressors based on diffraction gratings, followed by their compression through the agency of plane-parallel plates with positive dispersion. The hybrid laser system consists of a solid-state start-up laser complex generating femtosecond pulses, a KrF laser preamplifier, and a final amplifier.

A solid-state start-up facility emitting UV femtosecond pulses was designed and fabricated by Avesta-Project, a Russian company, in collaboration with researchers at FIAN. This facility, consisting of a 744-nm, 30-fs Ti:Sa laser, an optical stretcher, a regenerative amplifier, multi-pass amplifiers, an optical compressor, and a third-harmonic optical converter, emits 0.5-mJ, 60–100-fs pulses at 248 nm with a pulse repetition rate of 10 Hz. The laser beam diameter measures 8 mm. The maximum output radiation energy at the fundamental wavelength reaches 8 mJ. This facility can also generate 2-mJ second-harmonic femtosecond pulses at 372 nm. The electron-beam-pumped KrF laser preamplifier [27] has an active volume of $10 \times 10 \times 100$ cm^3. The final KrF laser amplifier [27] with an active volume of $16 \times 18 \times 100$ cm^3 is pumped by two counterpropagating electron beams generated by two electron guns and directed to a laser chamber through a titanium foil.

This hybrid laser setup was drawn in to study the amplification of ultrashort UV pulses in the two stages of electron-beam-pumped wide-aperture KrF amplifiers [28]. The total output energy of the preamplifier reached 23 mJ and the beam cross section area (38.5 cm^2) was about 60% of the preamplifier aperture. The ultrashort pulse energy at the final amplifier output amounted to 0.62 J under saturation conditions in a laser beam 92.5 cm^2 in cross-section area,

comprising 43% of the amplifier aperture. The input pulse incident on the preamplifier was ≈ 100 fs in duration, i.e. a stretcher was not used after beam exit from the start-up facility. The pulse duration at the final amplifier output, measured with an image-converter camera, did not exceed 1 ps and was no shorter than ≈ 330 fs (measurement of the coherence length). Thus, the pulse peak power reached ≈ 1 TW. The angular divergence of radiation was 20 μrad. Estimates show that, for an aperture filling factor equal to 1.0, the energy of the amplified pulse will reach ~ 1.5 J. The employment of a stretcher for the pulse of ≈ 60 fs in duration at the output of the start-up facility will provide laser pulses of $\sim 20-30$ TW in peak power at the system's output.

5. Interaction of femtosecond infrared and ultraviolet radiation pulses with matter

5.1 Filamentation of femtosecond pulses and ionization of gases by these pulses

The problem of amplification of ultrashort UV laser pulses in electron-beam KrF amplifiers proved to be closely related to processes of the nonlinear propagation of high-power UV laser pulses in the atmosphere, gases, and transmissive (transparent) optical elements. Experiments confirmed the existence of nonlinear absorption of comparatively low-intensity UV radiation, while investigations of the multiphoton ionization of pure gases (argon and nitrogen) [29] revealed that an increase in UV laser radiation intensity above 10^{12} W cm^{-2} leads to an increase in the number of photons participating in the nonlinear process from 3 to 4 quanta. It seems that this change is caused by a change in the ionization process. Thus, for low intensities (from $\approx 3 \times 10^{10}$ to 2×10^{11} W cm^{-2}), high-lying electron states are excited by three photons, and then one-photon ionization follows. As the radiation intensity is increased, the high-lying electron levels shift due to the dynamic Stark effect and 'exit' the three-photon resonance. As a result, nonresonance four-photon ionization is observed.

By using the method of time-resolved optical microscopy, researchers at the LGL have demonstrated the existence of a single or many short (down to 100 μm) and narrow (down to 5 μm in diameter) minifilaments of strongly focused ultrashort IR laser pulses in air [30]. The length of luminous plasma channels considerably exceeded the corresponding length of the focal waist. The plasma density estimated by various methods proved to be rather high (up to 10^{18} cm^{-3}). The existence of such minifilaments was previously subjected to question by leading researchers in this field, because earlier experimental examinations with weakly focused ultrashort pulses gave considerably greater lengths and diameters of gas (air) filaments (up to a few dozen meters and hundreds of micrometers, respectively). Numerical simulations for such conditions were performed at the Zuev Institute of Atmospheric Optics, SB RAS [31]. The results of numerical calculations confirmed the existence of mini-filaments produced by ultrashort pulses and also gave a systematic description of the fundamental mechanisms of producing minifilaments by strongly focused ultrashort pulses and their basic dimensional and energy parameters (the maximum intensity and plasma density in a filament).

Researchers at the LGL have performed a number of studies on the possibility of applications of minifilaments. Thus, experiments were performed on the generation of a third harmonic in air minifilaments. In particular, it was shown that the maximum conversion efficiency of strongly focused IR ultrashort pulses to third-harmonic UV ultrashort pulses could reach 0.16% [32]. The very strong focusing (numerical apertures of focusing optics down to 0.65) of laser pulses was used for the advancement of the innovation technology for microscale volume labeling of natural diamonds [by recording graphite microchannels; this work was performed in collaboration with the Kristall Industrial Association (Smolensk)] [33] and import-replacing medical technology for volume microscopic perforation of eye tissues for microsurgical vision correction by cornea shaping and nearly noninvasive removal of malignant tumors on the sclera (this work was performed in collaboration with the Central Clinical Hospital, RAS) [34]. Notice that practical technologies for microscopic labeling and eye microsurgery have been preceded by the fundamental studies into the physical mechanisms of producing microscopic damage in materials, and the peculiarities and parameters of microfilamentation in transparent media.

5.2 Nanophotonics of the nanostructured surfaces and bulk photonic crystals

Although the laser-induced fabrication of one-dimensional periodic surface nanostructures (PSNSs) under the action of ultrashort (femtosecond) laser pulses have been studied already for more than a decade, the PSNS fabrication mechanisms, in particular, dynamic changes in the optical properties of the optically excited surface of materials, the distribution of the electromagnetic field energy due to the interference of ultrashort pulses with a surface electromagnetic wave (SEW) excited by these pulses, mass transfer mechanisms (material removal due to ablation), the optics of a photoexcited nanostructured surface, and the appearance of subwavelength ($\Lambda \ll \lambda$, where λ and Λ are the wavelengths of the incident radiation and produced periodic structure, respectively) PSNSs have been investigated inadequately to date. Because of this, we examined the following main stages of the PSNS fabrication by ultrashort pulses [35–43]:

(1) the photoexcitation of a surface and interference of ultrashort pulses with SEWs subjected to IR and, for the first time, UV ultrashort pulses [35–37, 42];

(2) the appearance of the primary, as a rule, anharmonic, near-wavelength ($\Lambda \approx \lambda$) periodic nanorelief [35, 37];

(3) recording PSNSs (including subwavelength nanogratings) due to the diffraction of ultrashort pulses by the primary anharmonic nanorelief [35, 37, 38, 40–43];

(4) the fabrication of PSNSs during the interaction of multiple subsequent ultrashort pulses with a developed nanorelief, up to its degradation and formation of a microrelief [39–42].

A simple and informative method was proposed for studying the dynamic optical constants of matter on the ultrashort-pulse scale by measuring pulse self-reflection [35–37]. The higher harmonics of a nanorelief (up to the 7th harmonic) were observed for the first time [35, 37], and the fabrication of such subwavelength PSNSs was explained not by the unlikely generation of higher optical surface harmonics, but via the diffraction of ultrashort pulses by the primary anharmonic nanorelief (the superposition of nanorelief harmonics) which appears, as a rule, in a slightly above-threshold regime of nanostructuring, with the excitation of a set of SEWs with the corresponding wave-number spectrum [35, 37].

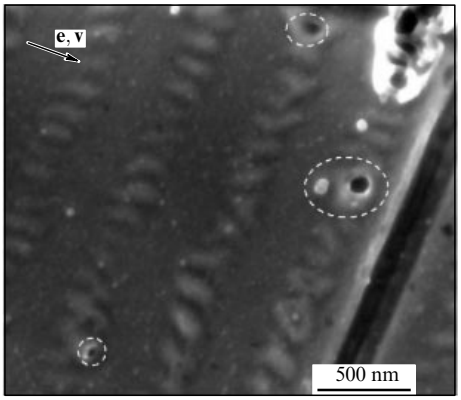

Figure 4. Nanostructures fabricated on an aluminium surface at the irradiation power density $F = 0.5$ J cm^{-2} and $N = 500$. The image was obtained with a scanning electron microscope with magnification 120,000. The arrow shows the direction of the polarization vector **e** of the laser field and the velocity vector **v** of a target. The dashed contours single out nanospikes with craters instead of a top and material removal traces.

In addition, the study of PSNS fabrication by ultrashort pulses with energy densities lying slightly below the threshold revealed not the regular sequences of nanorelief grooves but two-dimensional arrays of nanospikes (Fig. 4), the latter periodically appearing in the lines of the ultrashort-pulse–SEW interference maxima due to the cavitation instability of a surface melt [43] (the possibility of the formation of a nonperiodic nanorelief had been predicted earlier in calculations by the molecular dynamics method). The microscopic cavitation dynamics mechanism preceding the formation of nanospikes due to a partial 'frozen' split-off of a part of a surface melt film, as well as other microscopic mechanisms of the split-off and fragmentation ablations of solids under the action of ultrashort pulses, was first investigated by our team with the method of time-resolved optical microscopy in paper [44].

The results of this study demonstrated for the first time the possibility of monitoring the motion of the melting front in a material by observing acoustic reverberations in a surface melt film with the acoustic impedance different from the impedance of the solid material, and also the motion of the cavitation region from the surface to the melt volume caused by the surface cooling during its adiabatic expansion, followed by the split-off and extrusion of a cooled surface layer from the target surface on the subnanosecond time scale, probably mainly due to the vapor pressure in the cavitation region under the surface (nanofoam) rather than stress (rarefaction) waves circulating in the melt. Upon irradiation by ultrashort pulses with higher energy densities, we observed the irreversible fragmentation removal of a higher-temperature surface melt layer due to its cavitation.

The fragmentation mechanism of surface ablation of solid materials caused by ultrashort laser pulses and the higher-energy mechanism of their ablation via direct ionization were also examined by the method of contactless broadband ultrasonic diagnostics adapted for detecting superpower shock waves generated during ablation produced by above-mentioned pulses. It is known that during the propagation of superpower shock waves in materials, these materials experience plastic deformation (elastoplastic transition) and polymorphic transformations caused by the shock-wave loading. As a result, the profile of a propagating shock wave gradually changes, even in rather thin (submicron and micron thick) targets, which proves to be especially considerable in the case of generation of superpower shock waves during the ablation of targets caused by high-intensity ultrashort pulses with peak intensities up to 0.1–1 PW cm^{-2}. Because of this, we proposed a new approach to the study of superpower shock waves generated during the ablation of materials by high-intensity ultrashort laser pulses, which is based on the observation of the shock-wave evolution in a bordering medium with high shock-wave and optical strength, for example, in air [45].

We implemented the experimental scheme of recording superpower shock waves by the method of contactless broadband ultrasonic diagnostics by observing the propagation of shock waves *in air* from a surface being ablated to a broadband piezoelectric detector [45–47]. This scheme is devoid of the dimensional target-thickness effect and also allows one to investigate *in situ* a variety of materials with different surface reliefs with micrometer spatial resolution. We performed table-top investigations of superpower sub- and multimegabarn shock waves excited on an aluminium surface ablated in air under the action of high-intensity ($\leqslant 1$ PW cm^{-2}) linearly polarized ultrashort laser pulses [45]. The estimates of the initial pressure and velocity of a shock wave (the ablation torch) are in good agreement with data in the literature obtained by different methods for shock waves propagating *inside* a target being ablated (Fig. 5).

Finally, in the last years we have studied the production of sols of chemically 'pure' nanoparticles through the ablation of solid materials such as iron, gold, nickel, silicon, and a superconducting YbCo ceramic irradiated by ultrashort pulses in different liquids. Nanoparticle sols obtained in these experiments found application, in particular, to fabricate nanocomposites based on a three-dimensional photonic crystal dielectric matrix (artificial opal) by filling air nanovoids inside it with quantum dots-nanoparticles and then drying the solvent. The optical spectroscopy of the stop (forbidden) band of opal demonstrates, due to the high chemical purity of the nanoparticles, correct signs and high predictable amplitudes of the 'blue' (for metal nanoparticles) and 'red' (for dielectric nanoparticles) shifts of the band spectrum of the nanocomposite [48].

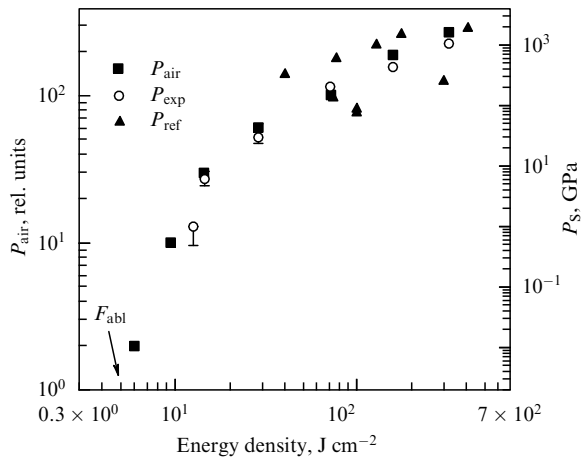

Figure 5. Experimental dependences of the pressure-wave amplitude P_{air} (left ordinate, dark squares) and the initial pressure P_S in the laser torch (right ordinate) on the irradiation energy density F: dots mark our experimental data P_{exp}, and triangles are data P_{ref} from the literature. The arrow shows the material ablation threshold F_{abl}.

5.3 Initiation of electric discharges by combined femtosecond and nanosecond UV laser pulses

Plasma channels produced by laser radiation in the atmospheric air or some other gases are of considerable interest for many fundamental problems and technological applications. Among them are the lightning initiation and active lightning protection, the directional transfer of microwave radiation to reduce its natural divergence, and laser acceleration of electrons. Unlike earlier experiments with submicrosecond CO_2 laser pulses [49], in which absorption in dense plasma produced during avalanche ionization restricted the channel length and continuity, new approaches with the aid of long UV pulses [50] or ultrashort femtosecond pulses [51] allow one to produce extended weakly ionized tracks in gases due to multiphoton ionization and (or) laser beam filamentation. Because primary electrons rapidly recombine with positive ions and attach to oxygen molecules for $\sim 10-50$ ns, it is reasonable to utilize additional visible or UV radiation to maintain the electron density at the desired level for a rather long time. Therefore, the combination of a train of ultrashort high-intense UV laser pulses with long UV pulses looks quite attractive for the production and subsequent maintenance of a plasma channel.

Within the framework of collaborative ISTC project No. 4073, the author and V D Zvorykin, A O Levchenko, S I Kudryashov, L V Seleznev, D V Sinitsyn, and N N Ustinovskii at the LGL developed a new optical scheme for a multistage hybrid Ti:Sa–KrF laser facility emitting trains of ultrashort pulses with a high peak power of 0.2–0.3 TW in combination with 100-ns high-energy pulses [52]. Single ultrashort pulses or a train of these pulses with a period of 5 ns were injected into an unstable confocal cavity of a main wide-aperture KrF-laser amplifier through a semitransparent meniscus, which were amplified in the course of multiple round trips in the cavity and overlapped with a free-running pulse (Fig. 6). The injected 0.5-mJ, 60-fs ultrashort laser pulses at 248.4 nm were generated by a Ti:Sa start-up facility and their energy was increased to ≈ 20 mJ in the KrF-laser preamplifier. The injected ultrashort pulses were amplified during multiple round trips in the cavity against the free-running generation background [their amplitude in Fig. 6 is 1000 times smaller than in reality because of the limited time resolution of a vacuum photodiode (≈ 1 ns) integrating signals of ultrashort pulses ≈ 1 ps in duration]. The energy of combined radiation pulses amounted to $\approx 10-30$ J. We measured the conductivity of plasma channels produced in the atmospheric air by combined UV pulses focused with a spherical mirror with a focal distance of ≈ 8.0 m. We detected a photocurrent signal caused by the electron component of photoionization plasma produced in the transfer region between two circular electrodes separated by a distance of 20 cm, the applied voltage being $U = 5-22$ kV.

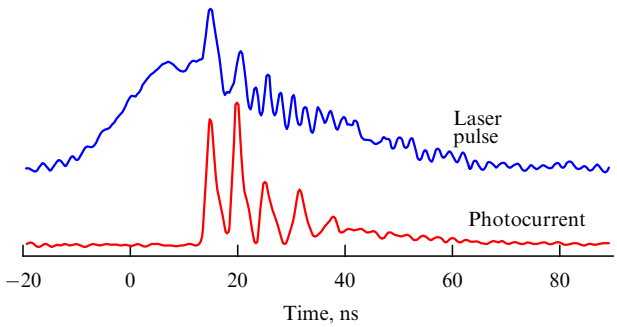

Figure 6. Oscillograms of a combined laser pulse (upper curve) and photocurrent (lower curve) during the injection of a train of ultrashort pulses into the laser cavity [52].

Typical oscillograms of a laser pulse detected with a photodiode (upper curve) and of an electron photocurrent (lower curve) in Fig. 6 show that the current amplitude, which is close to zero at the front of a free-running pulse, drastically increases with the appearance of an ultrashort pulse. The measurement of the electron photocurrent in the case of a 100-ns smooth pulse in the free-running mode (without the injection of ultrashort pulses) gave a photocurrent two orders of magnitude smaller than that in the case of a modulated laser pulse. This is explained by the nonlinear dependence of air photoionization on the laser radiation intensity. When the geometrical focus of the mirror was displaced within ≈ 1.0 m with respect to the interelectrode gap, the photocurrent changed insignificantly, which obviously indicates the filamentation of the ultrashort-pulse laser beam and allows one to estimate the nonlinear propagation length.

Preliminary experiments on the initiation of a breakdown in a discharge gap with a small length [53] showed that a free-running pulse produces electric breakdown in a gap 4.0 cm in length at the applied voltage of 50 kV, with the discharge pulse developing with a ≈ 5-μs delay with respect to the laser pulse, and its propagation direction being not determined by the laser beam. For the same applied voltage, a combined pulse with the same energy provides propagation of the discharge along the beam for a distance of 7 cm, with a delay at least two orders of magnitude smaller. The formation of an extended conducting channel with a comparatively high conductivity maintained by combined UV laser pulses for a few dozen nanoseconds suggests that it is possible to efficiently control a high-voltage breakdown in long air gaps.

6. Conclusion

High-power CO lasers developed in Russian institutions can be utilized for solving many practical problems, including laser uranium-isotope separation. To build a high-power electric-discharge oxygen–iodine laser in Russia, it is necessary to organize the corresponding research and development work. The first experiments with a hybrid terawatt femtosecond UV laser system built in Russia have shown that this system is promising for controling extended electric discharges. During the development of this laser system, we began to study the possibility of applications of femtosecond radiation in medicine and industry, and of changing the surface and bulk properties of solid materials.

References

1. Zarubin P V *Lazernoe Oruzhie — Mif ili Real'nost'? Moshchnye Lazery v SSSR i v Mire* (The Laser Weapon: A Myth or Reality? High-Power Lasers in the USSR and in the World) (Vladimir: OOO "Tranzit-Iks", 2009)
2. Korzhimanov A V et al. *Usp. Fiz. Nauk* **181** 9 (2011) [*Phys. Usp.* **54** 9 (2011)]
3. Ionin A et al. *AIP Conf. Proc.* **664** 697 (2003)
4. Ionin A A et al. *Proc. SPIE* **1397** 453 (1991)
5. Spalding I J et al. *Proc. SPIE* **2713** 103 (1996)
6. Walter S et al. *Kvantovaya Elektron.* **22** 833 (1995) [*Quantum Electron.* **25** 851 (1995)]

7. Beairsto C et al. *Kvantovaya Elektron.* **24** 631 (1997) [*Quantum Electron.* **27** 614 (1997)]
8. Ionin A A, Kleine K R F, Kobsa H *Proc. SPIE* **3092** 422 (1997)
9. Graves R M et al. *Proc. SPIE* **3885** 159 (2000)
10. Ionin A A, in *Gas Lasers* (Eds M Endo, R F Walter) (Boca Raton, Fl.: CRC Press/Taylor and Francis, 2007) p. 201
11. Basov N G et al. *IEEE J. Quantum Electron.* **36** 810 (2000)
12. Bohn W et al. *Kvantovaya Elektron.* **35** 1126 (2005) [*Quantum Electron.* **35** 1126 (2005)]
13. Ionin A A et al. *Laser Phys.* **20** 144 (2010)
14. Ionin A A et al. *IEEE J. Quantum Electron.* **45** 215 (2009)
15. Ionin A A et al. *Opt. Commun.* **282** 294 (2009)
16. Antonyuk E A et al., in *Lazery. Izmereniya. Informatsiya — 2011. Tezisy Dokladov 21-i Mezhdunarod. Konf., St. Petersburg, 7–9 Iyunya 2011 g.* (Proc. of the 21st Intern. Conf. on Lasers, Measurements, and Information, 7–9 June 2011. Abstracts of Papers) Vol. 3 (Ed. V E Privalov) (St. Petersburg: Izd. Politekhnicheskogo Univ., 2011) p. 8
17. Baranov V Yu et al., in *Izotopy: Svoistva, Poluchenie, Primenenie* (Isotopes: Their Properties, Production, and Application) Vol. 1 (Ed. V Yu Baranov) (Moscow: Fizmatlit, 2005) p. 474
18. Eerkens J W, in *Selected Papers on Laser Isotope Separation — Science and Technology* (Ed. J W Eerkens) (Bellingham, Wash.: SPIE Opt. Eng. Press, 1995) p. 531
19. Ionin A A et al. *Laser Phys. Lett.* **8** 723 (2011)
20. Andreev Yu M et al. *Opt. Zh.* **78** (2) 26 (2011) [*J. Opt. Technol.* **78** 102 (2011)]
21. Carroll D L et al. *Appl. Phys. Lett.* **86** 111104 (2005)
22. Ionin A A et al. *J. Phys. D Appl. Phys.* **40** R25 (2007)
23. Carroll D L et al. *Proc. SPIE* **8238** 823803 (2012)
24. Hecht J *Laser Focus World* (9) 41 (2011)
25. Ionin A A et al. *J. Phys. D Appl. Phys.* **36** 982 (2003)
26. Ionin À À et al. *Proc. SPIE* **7581** 758103 (2010)
27. Zvorykin V D et al. *Laser Part. Beams* **25** 435 (2007)
28. Zvorykin V D et al. *J. Phys. Conf. Ser.* **244** 032014 (2010)
29. Ionin A A et al. *Opt. Commun.* **282** 45 (2009)
30. Golosov E V et al. *Pis'ma Zh. Eksp. Teor. Fiz.* **90** 116 (2009) [*JETP Lett.* **90** 107 (2009)]
31. Geints Yu É et al. *Zh. Eksp. Teor. Fiz.* **138** 822 (2010) [*JETP* **111** 724 (2010)]
32. Ionin A A et al. *Laser Phys.* **21** 500 (2011)
33. Ionin A A et al. *Laser Phys.* **20** 1778 (2010)
34. Alekhin A A et al. *Laser Phys. Lett.* **7** 463 (2010)
35. Golosov E V et al. *Zh. Eksp. Teor. Fiz.* **140** 21 (2011) [*JETP* **113** 14 (2011)]
36. Golosov E V et al. *Ross. Nanotekhnol.* **6** (3–4) 82 (2011) [*Nanotechnol. Russia* **6** 237 (2011)]
37. Golosov E V et al. *Phys. Rev. B* **83** 115426 (2011)
38. Golosov E V et al. *Pis'ma Zh. Eksp. Teor. Fiz.* **90** 116 (2009) [*JETP Lett.* **90** 107 (2009)]
39. Golosov E V et al. *Fiz. Khim. Obr. Mater.* (2) 10 (2010)
40. Golosov E V et al. *Appl. Phys. A* **104** 701 (2011)
41. Ionin A A et al. *Kvantovaya Elektron.* **41** 829 (2011) [*Quantum Electron.* **41** 829 (2011)]
42. Korol'kov V P et al. *Kvantovaya Elektron.* **41** 387 (2011) [*Quantum Electron.* **41** 387 (2011)]
43. Ionin A A et al. *Pis'ma Zh. Eksp. Teor. Fiz.* **94** 289 (2011) [*JETP Lett.* **94** 266 (2011)]
44. Ionin A A et al. *Pis'ma Zh. Eksp. Teor. Fiz.* **94** 816 (2011) [*JETP Lett.* **94** 753 (2011)]
45. Ionin A A et al. *Pis'ma Zh. Eksp. Teor. Fiz.* **94** 35 (2011) [*JETP Lett.* **94** 34 (2011)]
46. Ionin A A, Kudryashov S I, Seleznev L V *Phys. Rev. E* **82** 016404 (2010)
47. Ionin A A, Kudryashov S I, Seleznev L V *Kratk. Soobshch. Fiz. FIAN* **38** (6) 13 (2011) [*Bull. Lebedev Phys. Inst.* **38** 161 (2011)]
48. Gorelik V S et al. *Kratk. Soobshch. Fiz. FIAN* **38** (11) 20 (2011) [*Bull. Lebedev Phys. Inst.* **38** 328 (2011)]
49. Koopman D V, Wilkenson T D *J. Appl. Phys.* **42** 1883 (1971)
50. Zhao X M et al. *IEEE J. Quantum Electron.* **31** 599 (1995)
51. Tzortzakis S et al. *Phys. Rev. E* **60** R3505 (1999)
52. Ionin A A et al. *Appl. Phys. Lett.* **100** 104105 (2012)
53. Ionin A A et al., in *High-Power Laser Ablation Conf. HPLA 2012, 28 April – 30 May 2012, Santa Fe, NM, USA, 2012*, HPLA Online Book of Procs.

PACS numbers: 14.60.St, **23.40.–s**, **31.10.+z**
DOI: 10.3367/UFNe.0182.201207i.0781

Laser radiation enhancement of forbidden orbital electron captures and of neutrinoless double electron captures by nuclei

M Yu Romanovskii

1. Introduction

The acceleration of the beta decay of particles (a process inverse to electron capture) under the action of an external electromagnetic field has been studied for more than four decades since the pioneering studies [1, 2]. The acceleration of nuclear beta decay was explained by the transformation of the wave function (WF) of a free emitted electron in a (high) electromagnetic field [3–7].[1] In this case, the intensity of an external electric field required for the several-fold acceleration of the process rate was estimated as $E_{\rm crit} = m_{\rm e}^2 c^3/e\hbar \sim 1.3 \times 10^{16}$ V cm^{-1} (where $m_{\rm e}$ is the electron mass, e is the elementary charge, c is the speed of light in vacuum, and $\hbar$ is the Planck constant).

The acceleration of the capture of orbital electrons (a process inverse to beta decay) has not yet drawn significant attention, partly because this effect has been known for a long time (e.g., the rate of the ^{7}Be $\to$ ^{7}Li process depends on the chemical bond involving a beryllium atom (see Ref. [8]). Furthermore, the theoretically and experimentally studied range of actions on the wave functions of orbital electrons was very wide. It covered the effects of the same chemical bonds and high pressure [9], the thermal effects (including superconductivity), the action of internal electric and magnetic fields of the medium, and plasma effects (see review [10]). K-electron capture was primarily considered, where the possible degree of rate acceleration did not exceed 10^{-2}. The known work (see, e.g., Refs [11–14]) on nuclear excitation accompanying electron transitions in the respective atoms was along the same lines.

The capture of electrons from atomic shells higher than the K-shell is also well known [15–17], including the capture of electrons with a nonzero orbital quantum number l [18, 19]. Just the latter process can be accelerated by an external

[1] Numerous incompletely accurate works predicting the acceleration of beta decay by comparatively moderate external fields are not mentioned here.

M Yu Romanovskii Prokhorov General Physics Institute, Russian Academy of Sciences, Moscow, Russian Federation
E-mail: slon@kapella.gpi.ru

Uspekhi Fizicheskikh Nauk **182** (7) 781–786 (2012)
DOI: 10.3367/UFNr.0182.201207i.0781
Translated by Yu V Morozov; edited by A Radzig